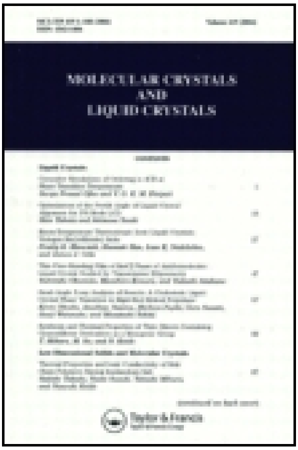

Molecular Crystals and Liquid Crystals Science and Technology. Section A. Molecular Crystals and Liquid Crystals

Publication details, including instructions for authors and subscription information:
http://www.tandfonline.com/loi/gmcl19

Structure and Mobility in Ferroelectric Liquid Crystalline Elastomers as Studied by Time-Resolved FTIR Spectroscopy

Holger Skupin [a], Sergej V. Shilov [b], Friedrich Kremer [a], Elisabeth Gebhard [c] & Rudolf Zentel [c]

[a] University of Leipzig, Abt. PAF, Linnéstr. 5, 04103, Leipzig

[b] Univ. of St. Petersburg, Inst. for Macromolecular Compounds

[c] BUGH Wuppertal, Inst. für Materialwissenschaften

To cite this article: Holger Skupin, Sergej V. Shilov, Friedrich Kremer, Elisabeth Gebhard & Rudolf Zentel (2001): Structure and Mobility in Ferroelectric Liquid Crystalline Elastomers as Studied by Time-Resolved FTIR Spectroscopy, Molecular Crystals and Liquid Crystals Science and Technology. Section A. Molecular Crystals and Liquid Crystals, 358:1, 37-51

To link to this article: http://dx.doi.org/10.1080/10587250108028269

Mol. Cryst. and Liq. Cryst., 2001, Vol. 358, pp. 37-51
Reprints available directly from the publisher
Photocopying permitted by license only

Published by license under the
Gordon and Breach Science Publishers imprint.
Printed in Malaysia

Structure and Mobility in Ferroelectric Liquid Crystalline Elastomers as Studied by Time-Resolved FTIR Spectroscopy

HOLGER SKUPIN[a], SERGEJ V. SHILOV[b], FRIEDRICH KREMER[a], ELISABETH GEBHARD[c] and RUDOLF ZENTEL[c]

[a]*University of Leipzig, Abt. PAF, Linnéstr. 5, 04103 Leipzig,* [b]*Univ. of St. Petersburg, Inst. for Macromolecular Compounds and* [c]*BUGH Wuppertal, Inst. für Materialwissenschaften*

The molecular structure and reorientation of ferroelectric liquid crystalline elastomers (FLCE) in response to an external electric field is studied on a microsecond scale with time-resolved Fourier transform infrared (FTIR) spectroscopy. In order to analyze the influence of the network on the molecular structure and mobility in FLCE, three similar FLC polysiloxanes are under study that differ just in their crosslinking architecture: besides the uncrosslinked polymer we obtain by photocrosslinking FLCE in which the backbones of either adjacent smectic layers ("interlayer") or of the same smectic layer ("intralayer") are preferably crosslinked. It is shown that the crosslinking leads to a slowing down of the molecular mobility which is stronger for the inter-than for the intralayer FLCE. Asymmetries in the reorientation times and/or in the reorientation angles are observed (elastic memory effect). The intralayer crosslinking causes a "locomotive effect": the reorientation of the mesogenic cores precedes that ofthe backbones.

Keywords: time resolved FTIR spectroscopy; ferroelectric liquid crystals; elastomeric networks

INTRODUCTION

Due to the combination of ferroelectricity and rubber elasticity ferroelectric liquid crystalline elastomers (FLCE) are a promising material for electroptical and piezoelectric applications [1-3]. The formation of network points during the thermal or photoinduced crosslinking process prohibits flow processes and enables piezoeffects as large as those of piezoceramics [4,5]. In order to study the influence of the crosslinking network on the structure and the mobility in response to an external electric field a homologues series of FLC polymers and elastomers is investigated by polarized time-resolved Fourier-transform infrared (FTIR) spectroscopy. Due to its specificity FTIR spectroscopy with polarized light can reveal the mean orientation and the orientation distribution of the different molecular segments of FLC [6-19], that are the mesogenic long axis, the polar (carbonyl) group, the alkyl tail and -in case of FLCP and FLCE- the polymeric backbone. By performing polarized FTIR with a time resolution of $\Delta t >= 5\mu s$ the reorientation dynamics in response to an external electric field can be studied in detail. By that one obtains for the different molecular segments the reorientation angles, the reorientation times, the reorientation path and the phase relation with respect to the external electric field [14-19].

As in most of the time resolved FTIR measurements the sample is hold fixed with respect to the infrared propagation vector, the obtained information about the evolution of the molecular orientation refers to the projection onto the plane normal to the beam propagation (this is the plane in which the polarizer is rotated). Therefore, conclusions about the reorientation dynamics are equivocal as long as the three-dimensional character of the reorientation path is not taken into account [17]. It is the aim of this paper to elucidate the segmental dynamics of FLCP and FLCE by deriving the reorientation paths in the 3D space and studying the time evolution of the mean orientations of the different segments along these reorientation paths.

In order to find out the influence of the elastomeric network on the segmental reorientation dynamics we investigated a homologous series of three FLCP/FLCE samples that have a similar chemical structure besides their different crosslinking architecture [20-23].

EXPERIMENTAL SETUP

The infrared spectra are measured with an FTIR spectrometer (FTS 6000, Bio-Rad) attached to an infrared microscope (UMA 500, Bio-Rad). The microscope can be operated in the visible light mode and in the infrared mode. In the visible mode the sample compartment is between two crossed polarizers which allows to position the FLC sample in the measurement spot of 100μm x 100 μm. In the infrared mode the polarization vector $\vec{\varepsilon}$ of the infrared beam can be varied by a rotatable wire-grid polarizer (figure 1).

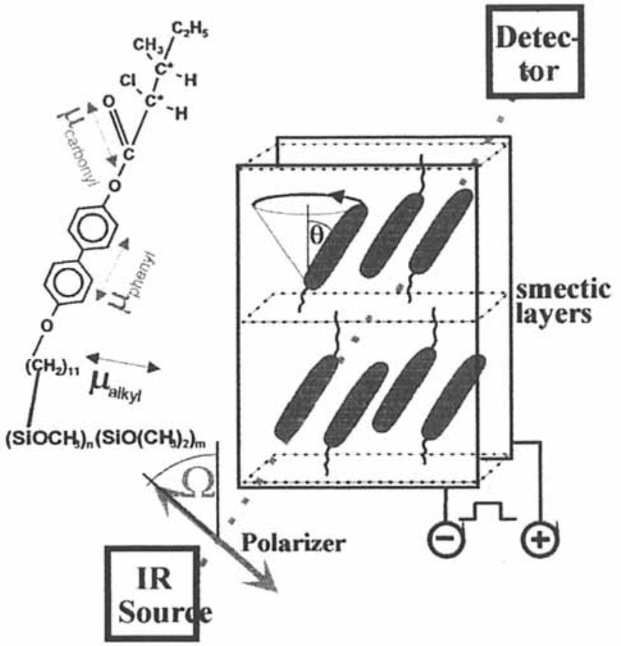

FIGURE 1 Experimental setup for the shear oriented FLC cells, the transition moments of the samples are indicated

A MCT (MercuryCadmiumTellurite) detector measures the infrared intensity in dependence of the optical retardation (which is the Fourier Transform of the spectral wavenumber ν), of the polarizer angle Ω and of the evolution time. The absorbance spectra for each polarizer angle Ω and time interval t is $A_{\Omega,t}(\nu) = -\ln(I_{\Omega,t}(\nu)/I^0_{\Omega}(\nu))$ where I and I^0 are the intensities in dependence of the variables Ω, t, ν measured with and without the sample placed in the beam. By use of the step-scan technique described elsewhere [14,15] a resolution in time of 5 µs can be obtained.

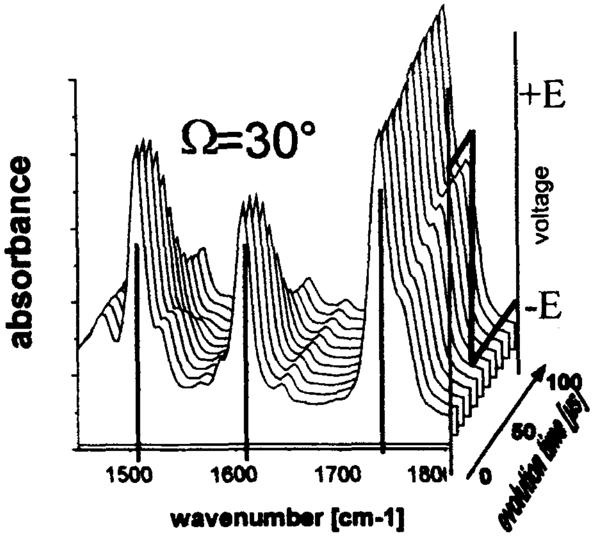

FIGURE 2 Evolution in time of bands assigned to the phenyl and the carbonyl group for a fixed polarizer angle Ω=30°. From the set of these time resolved spectra for each polarizer angle Ω=0°–180° the absorbance in dependence of Ω and t is derived for the different bands.

The samples under study are two FLC elastomers of a similar chemical structure but different crosslinking architecture and the corresponding uncrosslinked FLC polymer (Figures 4a,5a,6a). In the "inter"-layer crosslinked FLCE a photocrosslinkable group is attached at the terminal position of a mesogen which leads to the formation of three-dimensional networks. In contrast the functional group in the "intra"-layer FLCE is attached via a short spacer to the backbone, which leads to crosslinks lying preferably in the same backbone layer (two-dimensional network). Before crosslinking the samples are oriented by shearing between CaF_2 windows which are coated with an ITO layer in order to make the surface conductive. An additional SiO layer protects the ITO electrodes from short-circuits during the shearing. A 2μm PET foil separates the windows. These FLC cells are crosslinked about 5 degrees below the Sm-C*/Sm-A phase transition by UV-light. These cells are placed in the IR microscope with the incident light propagating normal to the CaF_2 windows (figure 1).

RESULTS AND DISCUSSION

For the analysis of the different infrared spectra the absorbance of the band maximums listed in Tab.1 are calculated with respect to an appropriate baseline.

TABLE1 Molecular assignment of the bands under study

Band name	wavenumber ν of the band maximum (cm^{-1})	Molecular group
Phenyl stretching	1499 and 1604	Mesogenic long axis
Carbonyl stretching	1730	carbonyl group
Asym. CH_2 stretching	2924	alkyl spacer
$Si-CH_3$ deformation	1261	polymeric backbone

By that for each of these four bands an array $A_\nu(\Omega,t)$ is obtained, where the index ν denotes one of the four band maximums. Each absorbance value A_ν of this array is proportional to the integral given in equation 1

$$A_v = \int (\bar{\mu}\bar{\varepsilon})^2 \, dV \ , \qquad (1)$$

where the polarization vector $\bar{\varepsilon}$ of the IR-light is a function of the polarizer angle Ω, $\bar{\mu}$ is the transition moment of the band ν which is time-dependent in its orientation and its orientation distribution function. The square of product $\bar{\mu}\cdot\bar{\varepsilon}$ is integrated for all transition moments in the measurement spot $\int dV$

Equation 1 describes an ellipsoid which is fully characterized by its three principle axes. The orientation of the principle axes of the absorbance ellipsoids denotes the average orientation of the corresponding transition moments and hence of the molecular groups assigned to them. It should be noted that the C2 symmetry axis must coincide with one of the principle axes of the ellipsoids. In the experiments presented in this paper the polarization vector is varied in the plane parallel to the cell windows. Therefore for a given time t any polarizer dependent absorbance $A_v(\Omega)$ can be fitted by the equation

$$A = -\log(P1 + P2\cos 2(\Omega - \Omega^{max})) , \qquad (2)$$

in which Ω^{max} denotes the polarizer angle for which maximal absorbance is measured. The maximal absorbance value is given by $A_{max} = -\log(P1 + P2)$ and the minimum absorbance is $A_{min} = -\log(P1 - P2)$. If the principle axis of the absorbance ellipsoid A_ζ is lying in the plane normal to the beam it is measured as A_{max}, if it is inclined to this plane smaller values for A_{max} are obtained (Fig 3a).

By that the value of Ω^{max}, A_{max} and A_ζ can be used to determine the average orientation of the different molecular groups in 3D-space. Fig. 3b shows the time evolution of Ω^{max} and A_{max} in response to the external electric field for the phenyl band of the intralayer crosslinked FLCE. $\Omega^{max}(t)$ describes how the principle axis of the phenyl band – being nearly parallel to the long mesogenic axis- reorients in the projection normal to the beam propagation.

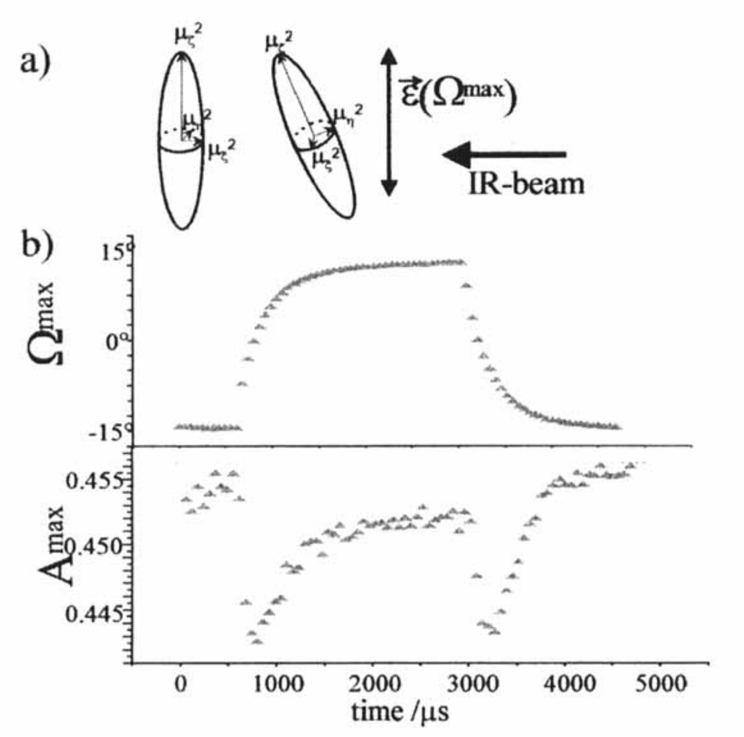

FIGURE 3 a) Sketch of the absorbance ellipsoid changing its inclination with respect to the plane normal to the infrared beam. b) Rotation on the tilt cone of the mesogenic long axis as observed as the evolution of the value and the polarizer angle of maximum phenyl absorbance

The evolution of the mesogen inclination with respect to this plane is reflected by the dips in the $A_{max}(t)$ curves. The combination of both curves proof that the mesogen reorientation takes place on a tilt cone. The reorientation on the tilt cones in the SmC* phase is also confirmed for the carbonyl group and the alkyl spacers. In contrast to that the reorientation of the backbones does not take place on the cone. Taking into account that the δ(Si-CH_3) transition moments are approximately isotropically distributed around the polymer backbone chain the two long principle axes of the δ(Si-CH_3) absorbance ellipsoid have about the same length and the preferred orientation of the backbones is about parallel to the short principle axis of this aborbance ellipsoid. During the electrical induced reorientation this short axis stays in the windows plane thus proving that the preferred orientation of the polymer backbones does not rotate around the layer normal as it is observed for the other molecular segments.

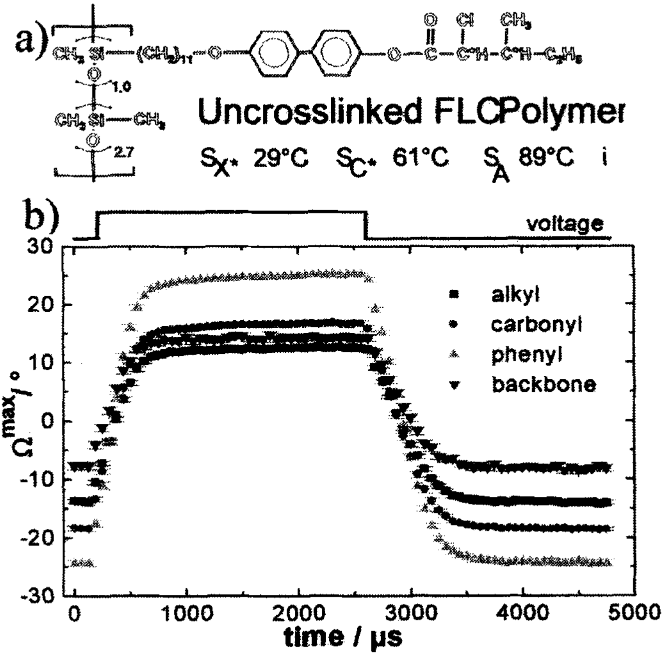

FIGURE 4 a) Chemical structure of the uncrosslinked FLC Polymer b) Evolution in time for the polarizer angle of extremum absorbance for the different bands, T=55°C (Sm-C*)

The finding of different reorientation paths of the segments enable a detailed analysis of the $\Omega^{max}(t)$ curves of the samples under study. For each sample different reorientation angles $\Omega^{max}(E>0) - \Omega^{max}(E<0)$ are observed for the phenyl, the alkyl, the carbonyl and the band assigned to the backbone (figures 4-6). With exception of the latter band these values equal twice the tilt angle of the corresponding tilt cone. The smaller tilt of the alkyl spacer shows that these chains decouple the reorientation of the mesogen from the polymeric backbones. The different tilt of the carbonyl and the mesogen proves that the distribution function of the carbonyl groups is not symmetric to the long mesogenic axis. This biased rotation of the carbonyl around the long mesogenic axis is the major molecular origin of the macroscopic spontaneous polarization of these ferroelectric samples [24].

Figures 4-6 show that the backbone also takes place in the reorientation process. As the preferred polymer backbone orientation was observed to stay in the plane, the observed change in Ω^{max} for the Si-CH_3-band has to be assigned to changes in the conformation of the polymer backbone which lead to a break of the rotational symmetry of the distribution of the δ(Si-CH_3) transition moments. The in-plane rotation of smectic layers are excluded as explanation for the shift of Ω^{max} for the Si-CH_3-band as these usually take place on a much larger time scale than that in our experiments. The reorientation time of the different molecular segments in the uncrosslinked FLC polymer for the rectangular pulsed electric field of $E=2.5$ V / μm is approximately 0.5 ms.

The reorientation times in the "interlayer" crosslinked sample (figure 5) are increased by a factor of about 2 with respect to the uncrosslinked FLCP although electric fields 10 times higher are applied. Hence the rotational viscosity in the interlayercrosslinked FLCE is about 20 times larger than in the uncrosslinked FLCP. In contrast to the FLCP an asymmetry in the switching times is observed. The crosslinking in the Sm-C* phase at negative field polarity leads to an elastic potential which supports the switching back into the molecular orientation that was fixed by the crosslinking and which hinders the reorientation in the opposite direction. The reorientation angles are reduced compared to the uncrosslinked FLCP. This is due to the fact that crosslinking took place in the Sm-C* phase near the Sm-A transition. The corresponding elastic potential hinders the thermal induced increase of the tilt angles of the molecular segments.

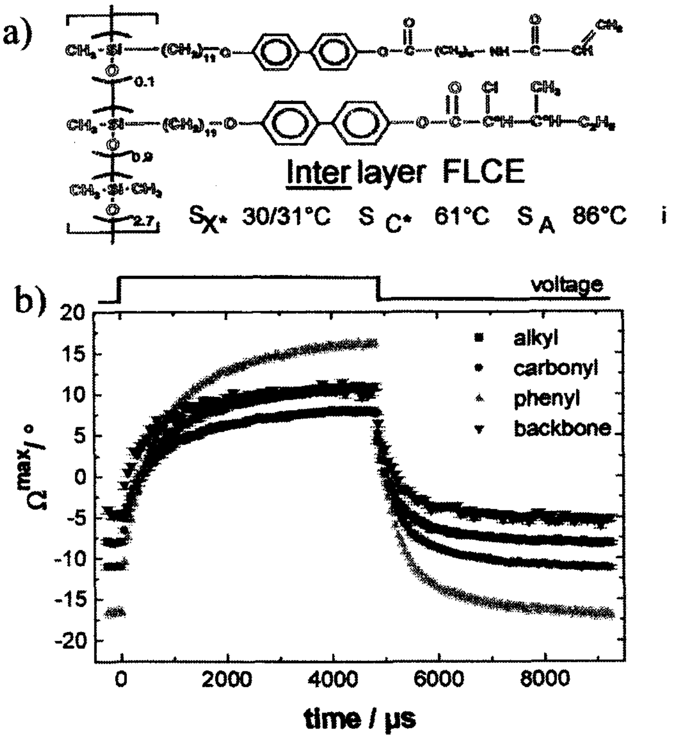

FIGURE 5 a) Chemical structure for the "interlayer" crosslinked FLC Elastomer b) Evolution in time for the polarizer angle of extremum absorbance for the different bands, T=55°C (Sm-C*)

A further asymmetry in the reorientation behavior can be observed on the angular axis. While for a negative field polarity the band assigned to the backbone shows the smallest Ω^{max} value, it exceeds for the

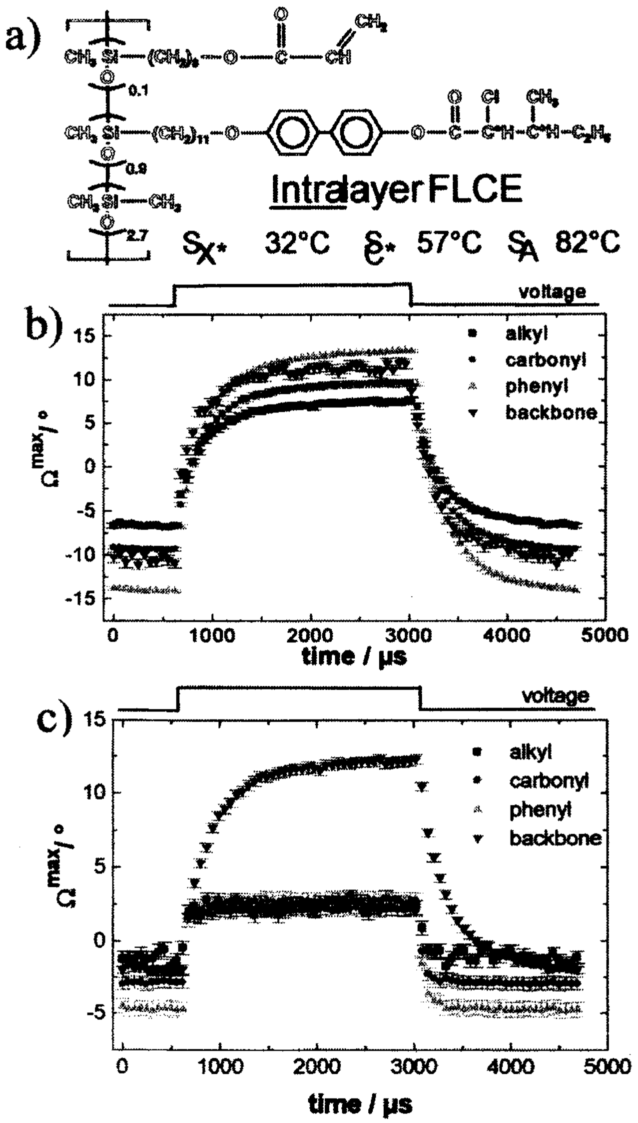

FIGURE 6 a) Chemical composition and sketch of the structure for the "intralayer" crosslinked FLC Elastomer b) Evolution in time for the polarizer angle of extremum absorbance for the different bands, at T=53°C (Sm-C*) and c) at T=65°C (Sm-A) positive polarity the Ω^{max} value of the alkyl and the carbonyl band. This elastic memory effect shows that the elastic potential has a strong influence on the ability of the backbone to change its conformation in response to the reorientation of the attached mesogens.

In the "intralayer" crosslinked FLCE (figure 6b) the rotational viscosity is less reduced than for the "interlayer" crosslinking, shorter reorientation times are measured in the Sm-C* phase. No asymmetries in the reorientation of the segments is observed: the two-dimensional network does not cause an elastic memory effect. The band assigned to the backbones exhibit in the "intralayer" crosslinked FLCE the second largest reorientation angles of the four bands under study. This shows that this network, formed preferably in the microphase separated backbone layer affects strongly the ability of the backbones to change their conformation. In the Sm-A phase of the "intralayer" crosslinked FLCE (figure 6c) the reorientation of the mesogen is about seven times faster than that of the backbones. The crosslinking does not allow conformational changes of the backbone in the time scale of fast electroclinic switching. The reorientation angles for the backbone exceed those of the mesogens which indicates that large conformational changes in these crosslinked backbone layers are necessary to compensate for the alteration of the molecular structure during the electroclinic switching.

TABLE 2 Reorientation times τ and reorientation angles $\Delta\Omega^{max}$ for the samples under study

Sample	$\tau_{(-E\ to\ +E)}$	$\tau_{(+E\ to\ -E)}$	$\Delta\Omega^{max}$ (phenyl)	$\Delta\Omega^{max}$ ($SiCH_3$)
Uncrosslinked FLCP,Sm-C*	0.5 ms	0.5 ms	50°	21°
"Interlayer" FLCE,Sm-C*	3.5 ms	2.5 ms	35°	15°
"Intralayer" FLCE,Sm-C*	1 ms	1 ms	28°	24°
"Intralayer" FLCE,Sm-A (backbone 1 ms)	0.15 ms	0.15 ms	8°	14°

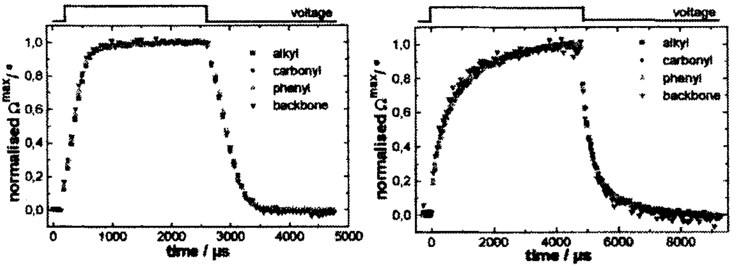

a) uncrosslinked FLCP,Sm-C* b)" interlayer" FLCE,Sm-C*

c) "intralayer" FLCE,Sm-C* d)" intralayer" FLCE,Sm-A

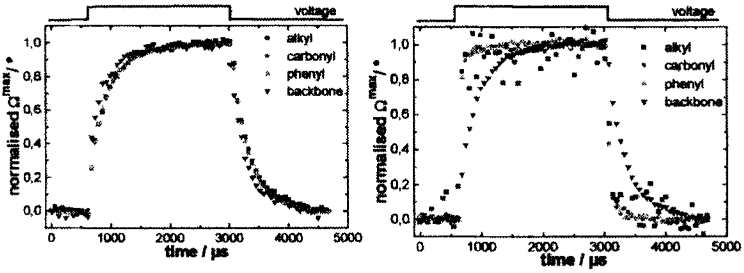

FIGURE 7 Normalized evolution in time for the polarizer angle of extremum absorbance for the different bands as derived from figures 4-6: a) uncrosslinked FLCP, Sm-C*, b) "inter-layer" crosslinked FLCE, Sm-C*, c) "intralayer" crosslinked FLCE, Sm-C*, d) "intralayer" crosslinked FLCE, Sm-A

The normalization of the $\Omega^{max}(t)$ curves for the Sm-C* phase of each of the different FLC samples lead to coincident plots (figures 7a-c). This shows the synchronous reorientation of the different segments on the time scale of the experiments. The normalized plot for the Sm-A phase (figure 7d) of the "intralayer" crosslinked FLCE reflects the asynchronous reorientation behavior between the backbone and the other molecular groups.

CONCLUSION

The capability of time-resolved Fourier transform infrared spectroscopy with polarized light is used to study the dynamics of a series of FLC polymers and elastomers that are similar besides their crosslinking architecture. Due to the specificity of infrared spectroscopy the reorientation of the different molecular segments can be followed in 3-D space. The crosslinking of the polymer precursor increases the rotational viscosity and leads to smaller tilt angles compared to the uncrosslinked FLCP. The crosslinking of backbones lying in adjacent smectic layers results in an elastic memory effect and hence in different reorientation times for the two directions of the field reversal. This interlayer crosslinking also causes a break in symmetry for the mutual arrangements between the mesogens and the backbone for the electric fields of opposite polarity. If the crosslinking takes place within the same microphase separated backbone layer an elastic memory effect is not observed. This intralayer crosslinking leads to large conformational changes of the backbone in response to the electrical induced mesogen reorientation. During the electroclinic switching the conformation of the backbone is changed too slowly to be synchronous with the mesogenic motion.

Acknowledgments

Support for H.S. by the Innovationskolleg „Phänomene an den Miniaturisierungsgrenzen“ and for S.V.S. by the Alexander von Humboldt foundation is gratefully acknowledged.

References

[1] R. Zentel; *Angew. Chem. Adv.Mater.,* **101,** 1437 (1989).

[2] U. Vallerien, F. Kremer, E.W. Fischer, H. Kapitza, R. Zentel, H. Poths; *Macromol. Chem., Rapid. Commun.*, **11,** 593 (1990).

[3] W. Meier, H. Finkelmann; *Macromol. Chem. Rapid. Commun.*, **11,** 599 (1990).

[4] T. Eckert; H. Finkelmann, M. Keck, W. Lehmann, F. Kremer, *Macromol. Rap. Commun.,* **17,** 767 (1996).

[5] W. Lehmann, P. Gattinger, M. Keck, F. Kremer, P. Stein, T. Eckert, H. Finkelmann, *Ferroelectrics* **208–209,** 373 (1998).

[6] K.H. Kim, K. Ishikawa, H. Takezoe, A. Fukuda, *Phys. Rev. E.* **51,** 2166 (1995).

[7] K. Miyachi, J. Matsushima, Y. Takanishi, K. Ishikawa, H. Takezoe, A. Fukuda, *Phys. Rev. E,* **52,** R2153(1995).

[8] K. Masutani, A. Yokota, Y. Furukawa, M. Tasumi, A. Yoshizawa, *Appl. Spectrosc.,* **47,** 1370 (1993).

[9] F. Hide, N.A. Clark, K Nito, A. Yasuda, D.M. Walba, *Phys. Rev. Lett.,* **75,** 2344 (1995).

[10] A. Kocot, R. Wrzalik, J.K. Vij, *Liq. Cryst.,* **21,** 147 (1996).

[11] A. Kocot, G. Kruk, R. Wrzalik, J.K. Vij, *Liq. Cryst.,* **12,** 1005 (1992).

[12] S.V. Shilov, S. Okretic, H.W. Siesler, *Vibrational Spectrosc.,* **9,** 57 (1995).

[13] S.V. Shilov, S. Okretic, H.W. Siesler, R. Zentel, T. Öge, *Macromol. Chem. Rap. Comm.* **16,** 125 (1995).
[14] S.V. Shilov, H. Skupin, F. Kremer, E. Gebhard, R. Zentel, *Liq. Cryst.* **22,** 203 (1997).
[15] S.V. Shilov, H. Skupin, F. Kremer, T. Wittig, R. Zentel, *Phys. Rev. Lett.* **79,** No.9, 1686 (1997).
[16] S.V. Shilov, H. Skupin, F. Kremer, T. Wittig, R. Zentel, *Macromol. Symp.,* **119,** 261 (1997).
[17] H. Skupin, F. Kremer, S.V. Shilov, P. Stein, H. Finkelmann, *Macromolecules,* **32,** 3746 (1999).
[18] H. Skupin, F. Kremer, S.V. Shilov, E. Gebhard, R. Zentel, *Mol. Cryst. Liq. Cryst.* **328,** 333 (1999).
[19] A. Merenga, S.V. Shilov, F. Kremer, Ch. Ober, *Macromolecules,* in press (1999).
[20] M. Brehmer, R. Zentel, F. Gießelmann, R. Germer, P. Zugenmaier, *Liq. Cryst.,* **21,** 589 (1996).
[21] E. Gebhard, M. Brehmer, R. Zentel, J. Reibel, G. Decher, H.M. Brodowsky, F. Kremer, In *The Wiley Polymer Networks Group Review;*K. te Nijenhuis, W. Mijs, Eds.: John Wiley Sons Ltd.: Chichester, Vol. 1 (1997).
[22] H.M. Brodowsky, U.-C. Boehnke, F. Kremer, E. Gebhard, R. Zentel, *Langmuir,* **13,** 5378 (1997).
[23] H.M. Brodowsky, U.-C. Boehnke, F. Kremer, E. Gebhard, R. Zentel, *Langmuir,* **15,** 274 (1999).
[24] A. Schönfeld, F. Kremer, *Ber. Bunsenges. Phys. Chem.,* **97,** 1237 (1993).